Chapter 1

PHYSICAL PRINCIPLES OF EFFICIENT EXCITATION TRANSFER IN LIGHT HARVESTING

Melih K. Şener and Klaus Schulten

After light absorption the primary process in light harvesting is the transfer of excitation to a reaction center which facilitates a separation of charge across a cell membrane. The physical principles underlying excitation transfer are explained. Theoretical methods for the description of the excitation migration process, including an expansion for excitation lifetime in terms of repeated trapping and subsequent detrapping events and the construction of representative pathways for excitation transfer based on mean first passage times, are presented. Measures for robustness and optimality of excitation transfer in terms of quantum yield are introduced. Photosystem I (PSI) is used as an example to illustrate the methods discussed. Some conclusions for the design of artificial light harvesting systems are also discussed.

Keywords: Photosynthesis, photosystem I, excitation transfer, quantum yield, mean first passage times, robustness, optimality.

1. INTRODUCTION

As the primary source of energy in the biosphere, photosynthesis is a process by which the energy of a photon is converted into increasingly more stable energy forms, first in the form of an electronic excitation of a pigment, followed by a charge separation across the cell membrane, and finally in the form of stable chemical bonds. In order to facilitate this process in an efficient manner photosynthetic systems share some common features despite the wide variety of their actual structures (Blankenship, 2002; van Amerongen *et al*., 2000).
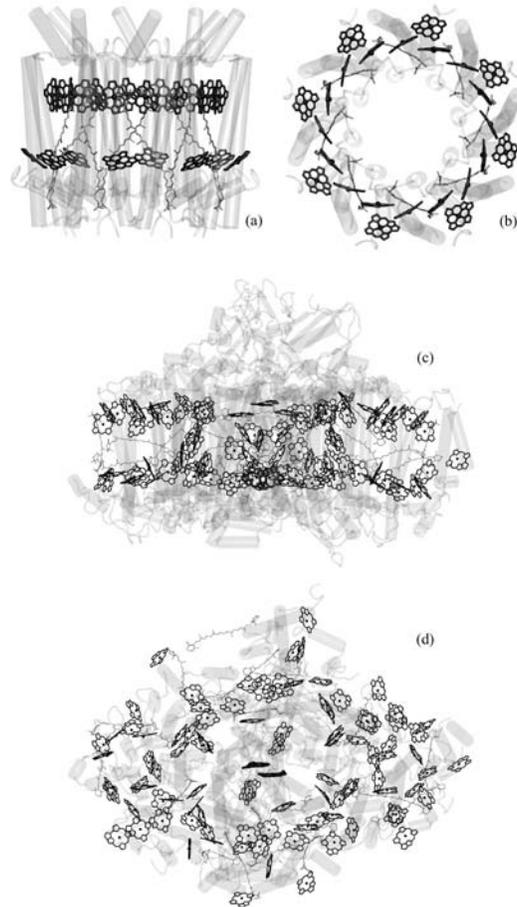
Fig 1. Comparison of two protein-pigment complexes used in light harvesting. Peripheral light harvesting complex LH2 from the purple bacterium *Rhodospirillum molischianum*: (a) side view (from the plane of the membrane), (b) top view (normal to the plane of the membrane). Photosystem I from the cyanobacterium *Synechococcus elongatus*: (c) side view, (d) top view. Unlike LH2, PSI contains also an electron transfer chain (not shown). For both systems the protein is rendered in transparent cartoon representation, the carotenoids are shown in gray and the (bacterio-)chlorophylls are shown in black represented by their porphyrin rings. Other cofactors are not shown for simplicity. Figure made using Protein Data Bank files 1LGH and 1JB0 with the program VMD (Humphrey *et al.,* 1996).

Pigments are the primary components of a light harvesting system, responsible for converting the energy of an absorbed photon into an electronic excitation. This excitation energy is then used for the transport of an electron across the cell membrane resulting in a voltage gradient. Most pigments are not directly involved in the charge separation process; instead their excitation energy is transferred eventually to a reaction center which facilitates the charge transfer. Thus, a light harvesting system typically comprises an array of peripheral antenna pigments surrounding a reaction center. These pigments might be located in separate antenna complexes excitonically coupled to the reaction center core, or they may constitute parts of a fused photosystem containing both a network of peripheral pigments and a reaction center.

In contrast to reaction center cores, antenna complexes display an amazing diversity (Blankenship, 2002). A typical example of an antenna complex is the peripheral light harvesting complex LH2 of the (anoxygenic) purple bacterial photosynthetic unit (Koepke *et al*., 1996; Hu *et al*., 2002), whereas an example of a fused photosystem is given by photosystem I (PSI), one of the two such major reaction center complexes used in oxygenic photosynthesis. The structure of PSI has recently been determined crystallographically in cyanobacteria (Jordan *et al*., 2001) and in higher plants (Ben-Shem *et al*., 2003). It is of interest to contrast LH2 with PSI (see Fig. 1). LH2 contains 24 bacterio-chlorophylls and 8 carotenoids arranged in a cylindrically symmetric fashion vs. 96 chlorophylls and 22 carotenoids found in cyanobacterial PSI with no obvious symmetry. PSI also contains additional cofactors forming an electron transfer chain. The uniform distribution of carotenoids in both structures is indicative of their photoprotective role. The anoxygenic purple bacterial light harvesting apparatus is known to have evolved earlier than the oxygenic light harvesting systems employed by cyanobacteria and plants (Xiong *et al*., 2000; Blankenship, 2001) indicating a trend for increased complexity.

A comparison of cyanobacterial and plant PSI structures (Ben-Shem *et al*., 2003) reveals a high degree of conservation in the geometry of the two chlorophyll networks (see Fig. 2). Except for an additional ten chlorophylls providing connections to the LHCI belt in plants (which is absent in cyanobacteria), the position and orientation of most of the

chlorophylls are conserved between the two structures. This is especially interesting, as chloroplasts in plants are believed to have diverged from cyanobacteria at least 1 billion years ago. The degree of conservation of the chlorophyll network after such a long period of independent evolution raises a question as to whether the geometry of the chlorophyll network of PSI had reached a point of optimality in terms of facilitating efficient excitation transfer prior to the divergence of the two structures.

Fig 2. Comparison of the chlorophyll networks in PSI from cyanobacteria (*Synechococcus elongatus)* represented as black lines and the higher plants (*Pisum sativum* var. alaska) represented as transparent gray bonds. The chlorophylls corresponding to the LHCI belt are not shown for plant PSI (see Fig. 5). Figure made using Protein Data Bank files 1JB0 and 1QZV with the program VMD.

The excitation energy absorbed by peripheral pigments migrates to a reaction center in a sequence of resonant energy transfers via intermediate pigments. Sufficiently strong couplings and significant

spectral overlap between pairs of pigments are essential for the efficient transfer of energy before the excitation is lost to dissipative processes. The excitation travels in a funnel-like fashion generally proceeding from higher energy pigments to lower energy ones. This is not always true, however, as PSI is known to contain chlorophylls that absorb light at longer wavelengths than the reaction center chlorophylls. These so-called 'red chlorophylls' are likely responsible for extending the spectral absorption profile of the complex. Spectral broadening of the pigment lineshapes due to thermal disorder makes it possible to have spectral overlap between pigments of varying energies. In fact, at lower temperatures the overall efficiency of the excitation migration process can drop significantly due to loss of resonance between neighboring pigments. Thus, thermal disorder constitutes an important ingredient for efficient excitation transfer in a light harvesting system with a broad spectral profile.

The presence and significance of thermal disorder in what is essentially a quantum mechanical process provides unique challenges for the study of excitation migration. Of the two of the many possible approaches for describing thermal effects in light harvesting, one is a description of 'dynamic' disorder given in the context of the energy fluctuations of the pigments along a molecular dynamics trajectory (Damjanović *et al*., 2002a). Another possible description is that of 'static' disorder as given by a thermodynamic average over many realizations of a light harvesting system formulated in terms of random matrix theory (Şener *et al*., 2002a).

A further challenge is provided by light harvesting complexes that are formed by the aggregation of multiple subunits. The cyanobacterial PSI, for example, is sometimes found in a trimeric form (see Fig. 3) containing a total of 288 chlorophylls. Although the function of trimer formation is not yet fully understood, excitation sharing between individual monomers is found to be feasible in trimeric PSI (Şener *et al*., 2004). Furthermore, conditions of iron deficiency are known to induce certain cyanobacteria to form even larger light harvesting assemblies comprised of a trimeric PSI core surrounded by a ring of satellite complexes containing a total of nearly five hundred chlorophylls

increasing the number chlorophylls per reaction center by nearly 60% (Bibby *et al.*, 2001).
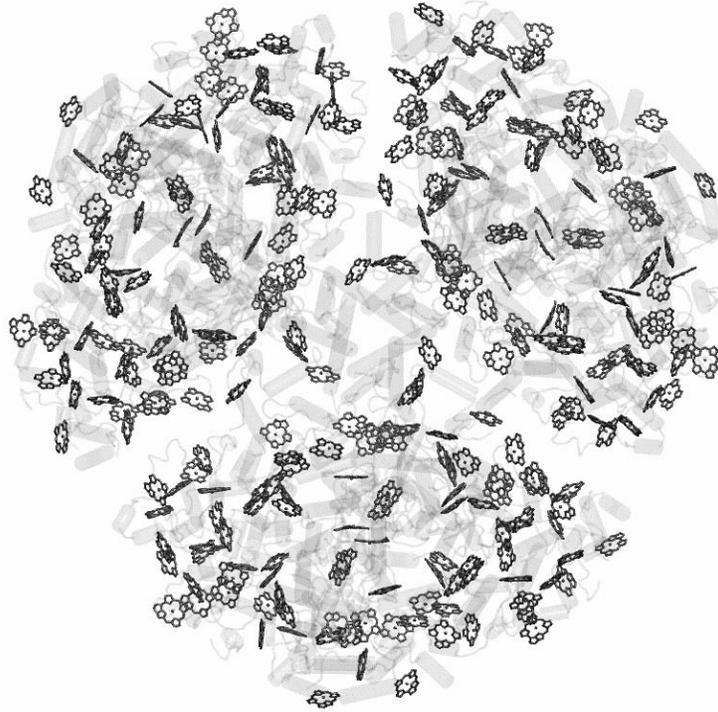
Fig 3. Trimeric form of PSI from the cyanobacterium *Synechococcus elongatus*. Chlorophylls are shown in black; other cofactors not shown for simplicity. The trimeric complex contains a total of 288 chlorophylls. Figure made using Protein Data Bank file 1JB0 with the program VMD.

The organization of this article is as follows: In the next section we introduce physical principles of excitation transfer based on Förster theory. In section 3 the average excitation lifetime and quantum yield are defined in terms of excitation transfer rates. In section 4 representative pathways of excitation migration are described in terms of mean first passage times to a reaction center. In section 5 an expansion method for

excitation migration in terms repeated trapping and detrapping events are introduced. In section 6 some measures of robustness and optimality of a pigment network are defined. Section 7 contains a discussion on principles for design of artificial light harvesting systems.

2. PRINCIPLES OF EXCITATION TRANSFER

In this section we introduce Förster theory as a basis of excitation transfer using an effective Hamiltonian formulation as a starting point as described in (Şener *et al*., 2002b). Under normal light conditions the flux of photons (~ 10 photons/chlorophyll/s) is sufficiently low that excitation migration in a pigment network can be satisfactorily modeled by single chlorophyll excitations. A basis set for an effective Hamiltonian can therefore be given in terms of exciton states where one pigment is at its lowest excited electronic state while all other pigments are in their ground state

$$|i> = |\phi_1 \phi_2 \cdots \phi_i^* \cdots \phi_N>, \quad i = 1, 2, \ldots, N. \tag{1}$$

Here N denotes the number of pigments; ϕ_i and ϕ_i^* denote the ground and first excited states of the ith pigment, respectively. For a chlorophyll molecule the lowest excited state is the so-called Q_y state (Scheer, 1991). In this basis set an effective Hamiltonian can be expressed as

$$H = \begin{pmatrix} \varepsilon_1 & H_{12} & \cdots & H_{1N} \\ H_{21} & \varepsilon_2 & \cdots & H_{12} \\ \vdots & \vdots & \ddots & \vdots \\ H_{N1} & H_{N2} & \cdots & \varepsilon_N \end{pmatrix}, \tag{2}$$

where ε_i denotes the excitation energy for pigment i and H_{ij} is the electronic coupling between pigments i and j. The coupling between two pigments has two contributions corresponding to a direct Coulomb term (Förster, 1948) and an electron exchange term (Dexter, 1953). For a typical network of chlorophylls as illustrated in the previous section the distance between a pair of chlorophylls is generally large enough that the exchange term is negligible and the coupling is dominated by the

Coulomb term (Damjanović *et al.*, 1999). In the lowest order approximation this coupling is

$$H_{ij} = C\left(\frac{\mathbf{d}_i \cdot \mathbf{d}_j}{r_{ij}^{\,3}} - \frac{3(\mathbf{r}_{ij} \cdot \mathbf{d}_i)(\mathbf{r}_{ij} \cdot \mathbf{d}_j)}{r_{ij}^{\,5}}\right), \tag{3}$$

where $\mathbf{d}_i$ is the unit vector along the transition dipole moment of pigment i, $\mathbf{r}_{ij}$ is the vector connecting the pigments i and j, and C is a constant. For the coupling of chlorophyll a molecules in PSI the prefactor in (3) is $C = 116\,000$ Å^3 cm^{-1}, where (as a customary abuse of notation) the energy is measured in terms of wavenumbers (1 cm^{-1} = 8066^{-1} eV).

The dipolar approximation given in (3) has the advantage of enabling the computation of the coupling between two chlorophylls simply from the knowledge of their relative spatial orientations. The direction of the transition dipole moment vector of the lowest excited (Q_y) state of a chlorophyll is approximately directed along a vector connecting the N_B and N_D atoms in the porphyrin ring of the chlorophyll and positioned at the central Mg atom (see Fig. 4). The dipolar approximation becomes increasingly less reliable as the inter-chlorophyll distance becomes smaller than 10 Å, in which case higher multipole contributions need to be taken into account (Damjanović *et al.*, 1999; Şener *et al.*, 2002b).

According to the Förster theory, the rate T_{ij} of transfer of excitation energy between two pigments, i and j, depends on their respective coupling H_{ij} as well as the spectral overlap J_{ij} between the emission spectrum S_i^D of the donor and the absorption spectrum S_j^A of the acceptor

$$T_{ij} = \frac{2\pi}{\hbar}\left|H_{ij}\right|^2 J_{ij}, \quad J_{ij} = \int S_i^D(E) S_j^A(E) dE. \tag{4}$$
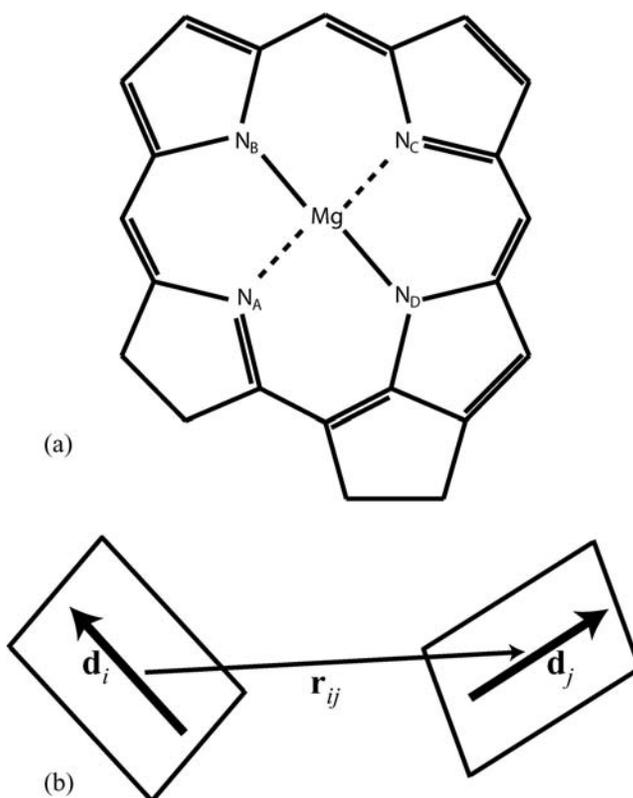
Fig 4. Geometry of chlorophyll interactions for dipolar approximation. (a) Porphyrin ring of a chlorophyll molecule. The transition dipole moment for the Q_y state is approximately along a vector connecting the N_B and N_D atoms. (b) Inter-chlorophyll coupling between two chlorophylls in the dipolar approximation is determined by their transition dipole moments $\mathbf{d}_i$ and the vector $\mathbf{r}_{ij}$ connecting their central Mg atoms (see Eq. 3).

Förster excitation transfer describes a nonradiative process and is applicable to weakly coupled pigments. Combining (3) and (4) it is seen that the transfer rate drops as $1/R^6$ over large distances. The Förster radius, defined to be the distance over which excitation transfer is 50% efficient, is about 80-90 Å for a pair of chlorophyll *a* molecules (Blankenship, 2002). Excitation transfer has typically a longer range than electron transfer which requires a direct overlap of electronic wave

functions of the two pigments. This has an important implication on the evolutionary design of reaction center cores: Antenna pigments are situated away from the immediate vicinity of the electron transfer chain to prevent loss of transported electrons while still enabling efficient excitation transfer to the reaction center.

The transition rate matrix T_{ij} as given in (4) can be used to create a map of excitation transfer pathways by illustrating the strongest connections between chlorophylls by increasingly thicker bonds (see Fig. 5). An excitation can then be viewed to follow a stochastic path along the connections until it is finally used up in a reaction center for charge separation or dissipated. Not surprisingly, a comparison of the excitation transfer pathways of cyanobacterial and plant PSI display remarkable similarities (except for the LHCI belt in the plant system) due to the conserved geometry of chlorophylls.

3. EXCITATION LIFETIME AND QUANTUM YIELD

The transfer rates T_{ij} between pigments can be used to describe the excitation migration process. Of particular interest are the average lifetime of an excitation after the initial absorption of a photon and the quantum yield, or efficiency, of the system, which is given by the probability of an excitation to cause charge separation as opposed to being dissipated. As we shall see shortly, typical quantum yields tend to be large (near unity) due to a separation of the dissipation (ns) and the excitation transfer and trapping (ps) time scales.

In order to formulate the excitation lifetime and the quantum yield in terms of transfer rates, we first introduce a master equation for the rate of change of occupation probabilities of chlorophylls. In the discussion below, a single excitation will be assumed to be localized at one of the chlorophylls and the effects of excitonic delocalization will be ignored. As a specific example we shall consider the case of excitation migration in cyanobacterial PSI (Şener *et al.*, 2002b; 2004).
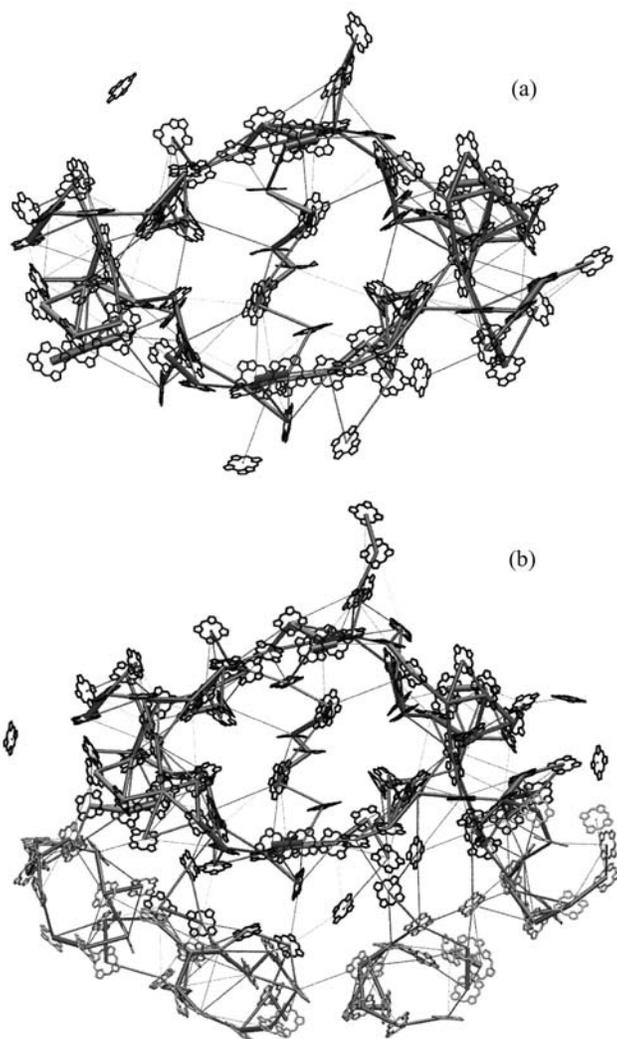
Fig 5. Connectivity of the chlorophyll networks in PSI from cyanobacteria (a) and higher plants (b). The thickness of a line between two chlorophylls is proportional to the logarithm of the excitation transfer rate between them. Only the strongest connections are shown for simplicity. Chlorophylls of the LHCI belt in plant PSI are rendered in gray in (b). Figure made using Protein Data Bank files 1JB0 and 1QZV with the program VMD.

Let $p_i(t)$ denote the probability of chlorophyll i being electronically excited at time t. The change in this probability is due to excitation transfer, dissipation, or charge separation events (if i is a charge separation site). The rate of change can be expressed as a master equation for the state vector $|p(t)\rangle = \sum_i p(i)|i\rangle$

$$\frac{d}{dt}|p(t)\rangle = K|p(t)\rangle,$$

$$K_{ij} = T_{ji} - \delta_{ij}\left(k_{CS}\delta_{i,CS} + k_{diss} + \sum_k T_{ik}\right),$$

(5)

where $k_{diss} = 1$ ns^{-1} is the dissipation rate, assumed to be uniform for all chlorophylls, $k_{CS} = 1$ ps^{-1} is the charge separation rate at the reaction center, and $\delta_{i,CS}$ is equal to one if i is a charge separation site and zero otherwise. The formal solution to Eq. (5) is

$$|p(t)\rangle = e^{Kt}|p(0)\rangle.$$

(6)

Let us denote by $n(t)$ the probability that there is still an excitation in the system at time t. One can express $n(t)$ as

$$n(t) = \sum_i p_i(t) = \sum_i \langle i|p(t)\rangle = \langle \mathbf{1}|p(t)\rangle,$$

(7)

where $|\mathbf{1}\rangle \equiv \sum_i |i\rangle$. Then the probability that the excitation disappears between t and $t + dt$ is given by $-\frac{d}{dt}n(t)dt$ and the expectation value of the excitation lifetime in the system is

$$\tau = -\int_0^\infty dt\, t\, \frac{d}{dt}n(t).$$

(8)

The quantum yield q of the system describing the probability of charge separation can also be expressed in a form similar to Eq. (8). The

probability that the excitation is used up for charge transfer between t and $t + dt$ is given by $k_{CS} \sum\limits_{i \in CS} \langle i | p(t) \rangle dt$. Thus, the quantum yield is

$$q = \int\limits_0^\infty dt\, k_{CS} \sum\limits_{i \in CS} \langle i | p(t) \rangle. \tag{9}$$

Eqs. (8) and (9) can be evaluated with the help of an identity for a matrix K with negative eigenvalues

$$\int\limits_0^\infty dt\, e^{Kt} = -K^{-1}. \tag{10}$$

Integrating Eq. (8) by parts and combining with Eqs. (6) and (10) we arrive at a final exact expression for average excitation lifetime

$$\tau = -\langle \mathbf{1} | K^{-1} | p(0) \rangle. \tag{11}$$

Similarly, combining Eqs. (9), (6), and (10) results in an expression for the quantum yield

$$q = -k_{CS} \sum\limits_{i \in CS} \langle i | K^{-1} | p(0) \rangle. \tag{12}$$

For the excitation transfer network of cyanobacterial PSI illustrated in Fig. 5(a) and for chlorophyll site energies as computed in (Damjanović *et al.*, 2002b), average excitation lifetime and quantum yield, computed from Eqs. (11) and (12), are $\tau = 32$ ps and $q = 0.97$, respectively. These values compare favorably with observations (the computed average excitation lifetime is an overestimate of the reported values of 20-25 ps) and do not change significantly between monomeric and trimeric forms of PSI (Şener *et al*., 2004).

It is important to emphasize that this structure based approach on studying excitation transfer dynamics contains no arbitrary parameters. Geometrical information about the chlorophyll network, combined with the application of basic physical principles of excitation transfer determines the values of all dynamical quantities. Thus, a comparison

with observation essentially provides a test for our understanding of the physics of the light harvesting process.

4. REPRESENTATIVE PATHWAYS OF EXCITATION TRANSFER BASED ON MEAN FIRST PASSAGE TIMES

A typical excitation migration event taking place over the network illustrated in Fig. 5 can contain hundreds of individual excitation transfer steps between pigments. Therefore, the random paths along which the excitation travels are not easy to visualize. A more intuitive picture of the way excitation energy is 'funneled' toward the reaction center can be constructed from paths of steepest descent based on mean first passage times of excitation from a pigment to a reaction center. Representative pathways of excitation transfer constructed in this manner are unidirectional and always terminate at a charge separation site (Park *et al*., 2003).

Let us denote the mean first passage time of an excitation located at chlorophyll *i* to a charge separation site by τ_i^{MFPT}. An expression for τ_i^{MFPT} can be constructed (Park *et al*., 2003) in terms of the matrix *K* appearing in Eq. (5):

$$\tau_i^{MFPT} = -\frac{1}{\phi_i}\sum_j \phi_j \left(K^{-1}\right)_{ji},$$

$$\phi_i \equiv -\sum_j \xi_j \left(K^{-1}\right)_{ji}, \tag{13}$$

$$\xi_i \equiv \sum_{j \in CS} K_{ji}.$$

In order to construct paths of steepest descent in the excitation transfer landscape, we regard the average excitation transfer time $1/T_{ij}$ from a chlorophyll *i* to a chlorophyll *j* as a measure of distance among the set of chlorophylls. Then the product $(\tau_i^{MFPT} - \tau_j^{MFPT})T_{ij}$ can be interpreted as the rate of descent in the value of the mean first passage time from chlorophyll *i* to chlorophyll *j*. Therefore, the path of steepest descent

from a chlorophyll i will go to a chlorophyll k only if the value of $(\tau_i^{MFPT} - \tau_j^{MFPT})T_{ij}$ is maximized for k.
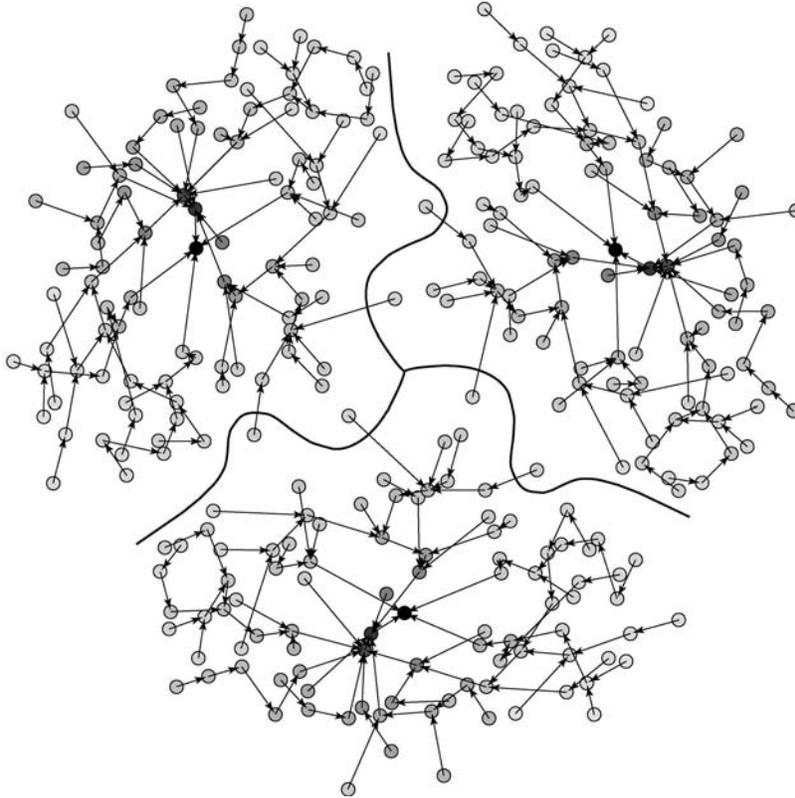
Fig 6. Representative pathways of excitation transfer based on mean first passage times to a reaction center for the chlorophyll network of trimeric cyanobacterial PSI. Chlorophylls are represented as circles; the tone of each circle denotes the mean first passage time of that chlorophyll in decreasing order from light gray to black. The partition divides the chlorophylls according to the PSI monomer they belong to. Thus, some chlorophylls near the inter-monomer boundary are functionally part of the neighboring PSI monomer instead of their own.

Fig. 6 illustrates the representative pathways thus constructed for the chlorophyll network of the trimeric cyanobacterial PSI. The pathways in

Fig. 6 split naturally into three disjoint sets. This is because each chlorophyll unidirectionally connects to only one other chlorophyll, and the three separate reaction centers of the individual monomers provide termination points for the pathways. Coincidentally, the three sets of chlorophylls defined by this partition do not coincide exactly with the sets of chlorophylls belonging to the same PSI monomer. This is because some chlorophylls near the boundary are more closely coupled to their neighboring monomer instead of their own. The division of the chlorophylls into disjoint sets in this manner does not imply the absence of excitation transfer between monomers. The stochastic path followed by an excitation may connect two chlorophylls on different sides of the inter-monomer boundary as long as they are coupled sufficiently strongly. In fact, a cross-monomer excitation trapping probability of about 40% was reported for the PSI trimer (Şener *et al*., 2004).

5. SOJOURN EXPANSION: AN EXPANSION FOR EXCITATION MIGRATION IN TERMS OF REPEATED DETRAPPING EVENTS

The excitation migration process does not necessarily terminate with the arrival of the excitation to a charge separation site. There is a finite probability, depending on the ratios of the charge separation rate and the total detrapping rate from the charge separation site, that the excitation will escape back to the chlorophylls in the periphery, only to migrate back again to a reaction center, if not dissipated first. Thus, the excitation migration process can be expanded naturally in terms of migration, trapping, and subsequent detrapping and retrapping events. Below we present such an expansion for the average excitation lifetime, called the sojourn expansion since it describes repeated return events to the reaction center (Şener *et al*., 2004).

Let us consider a network of N chlorophylls, M of which are charge separation sites, whose excitation transfer dynamics is described in terms of a master equation as in section 3. In order to expand Eq. (11) for the average excitation lifetime, we will separate from the matrix K in Eq. (5) the part that corresponds to detrapping processes.

Let the detrapping matrix Δ denote the part of the transfer matrix describing the detrapping events from the charge separation sites. The detrapping matrix Δ can be expressed in terms of the detrapping rates as

$$\Delta \equiv \sum_k \sum_{j \in CS} T_{jk} |k\rangle\langle j| = \sum_{j \in CS} W_{D,j} |T_j\rangle\langle j|,$$

$$W_{D,j} \equiv \sum_k Tjk, \quad j \in CS, \tag{14}$$

$$|T_j\rangle \equiv \frac{1}{W_{D,j}} \sum_k T_{jk} |k\rangle, \quad j \in CS,$$

where we have introduced the total detrapping rate W_{Dj} from a charge separation site j, and the transient state $|T_j\rangle$ describing the distribution of occupation probabilities immediately following a detrapping event at site j. Thus, we separate K into two parts as

$$K \equiv \kappa + \Delta, \tag{15}$$

which can be inverted to yield

$$K^{-1} = \kappa^{-1} - \kappa^{-1}\Delta\kappa^{-1} + \kappa^{-1}\Delta\kappa^{-1}\Delta\kappa^{-1} - \cdots. \tag{16}$$

Eqs. (11) and (16) can be combined to yield a series for the average excitation lifetime

$$\tau = \tau_0 + \tau_1 + \tau_2 + \cdots,$$

$$\tau_0 = -\langle \mathbf{1}|\kappa^{-1}|p(0)\rangle,$$

$$\tau_1 = \langle \mathbf{1}|\kappa^{-1}\Delta\kappa^{-1}|p(0)\rangle, \tag{17}$$

$$\tau_2 = -\langle \mathbf{1}|\kappa^{-1}\Delta\kappa^{-1}\Delta\kappa^{-1}|p(0)\rangle,$$

$$\vdots$$

The individual terms in the expansion in Eq. (17) can be evaluated explicitly using Eq. (14). For this purpose, we introduce the conditional detrapping probabilities at site j

$$(Q)_j \equiv -W_{D,j}\langle j|\kappa^{-1}|p(0)\rangle, \quad j \in CS, \tag{18}$$

for the initial condition given by $\left| p(0) \right\rangle$ and

$$(Q_T)_{jk} \equiv -W_{D,j}\left\langle j \left| \kappa^{-1} \right| T_k \right\rangle, \quad j,k \in CS, \qquad (19)$$

for the initial condition given by the transient state $\left| T_k \right\rangle$ following detrapping at site k. Additionally, we introduce the sojourn time

$$(T_{soj})_j \equiv -\left\langle \mathbf{1} \left| \kappa^{-1} \right| T_j \right\rangle, \quad j \in CS, \qquad (20)$$

as the average lifetime of an excitation immediately following a detrapping event at site j, but not involving any further detrapping events.

The terms Q and T_{soj} in Eqs. (18) and (20), respectively, form vectors of dimension M, whereas Q_T in Eq. (19) forms a matrix of dimension M. Using these quantities, the various terms in Eq. (17) can be evaluated in a succinct form:

$$
\begin{aligned}
\tau_1 &= T_{soj} \cdot Q, \\
\tau_2 &= T_{soj} \cdot Q_T \cdot Q, \\
\tau_3 &= T_{soj} \cdot Q_T^2 \cdot Q, \\
&\vdots
\end{aligned}
\qquad (21)
$$

where a dot indicates an interior product between vectors and matrices of dimension M. The convergence of this expansion is proved in (Şener *et al.*, 2004).

A final expression for the average excitation lifetime is obtained by explicitly summing the terms in Eq. (21)

$$\tau = \tau_0 + T_{soj} \cdot \left(1_M - Q_T\right)^{-1} \cdot Q, \qquad (22)$$

where 1_M denotes the identity matrix of size M.

As an application of the sojourn expansion to a light harvesting system with multiple reaction centers, we consider the trimeric PSI complex portrayed earlier. The trimeric symmetry results in a further simplification of Eq. (22), since the conditional probabilities $(Q)_j$ and

$(Q_T)_{jk}$ and the sojourn times $(T_{soj})_j$ given in Eqs. (18), (19), and (20) are invariant under a cyclic permutation of the labels. Thus, Eq. (22) can be rewritten for the case of the PSI trimer as

$$\tau = \tau_0 + \frac{3(Q)_1(T_{soj})_1}{1-(Q_T)_{11}-(Q_T)_{12}-(Q_T)_{13}} .$$

<div align="right">(23)</div>

The terms appearing in Eq. (23) are given in Table 1. It is seen that nearly 40% of the total lifetime stems from repeated detrapping events.

Table 1. Coefficients of the sojourn expansion, Eq. (23), for trimeric PSI.

τ	τ_0	$(T_{soj})_1$	$(Q)_1$	$(Q_T)_{11}$	$(Q_T)_{12}$	$(Q_T)_{13}$
32 ps	19 ps	7.5ps	0.21	0.563	0.037	0.037

6. ROBUSTNESS AND OPTIMALITY OF A LIGHT HARVESTING SYSTEM

Environmental change and competition are two major challenges that all biological systems must cope with. Adaptability to changing external conditions, or *robustness*, of a system typically manifests itself in terms of a parameter insensitivity of its dynamics and a graceful degradation of its components. Competition, on the other hand, drives a system towards *optimality*, as a less efficient system will find itself at an evolutionary disadvantage.

It is very difficult to quantify robustness and optimality in general terms for an arbitrary biological system since the fitness landscape over which adaptability needs to be judged is enormously complex. A light harvesting system, however, provides a natural, if somewhat crude, measure of its efficiency in terms of the quantum yield of the excitation migration process. It is a simple matter to model the effects of various perturbations, such as thermal disorder or loss of individual components, on the quantum yield. Similarly, questions regarding the optimality of the geometry of the chlorophyll network can be investigated by generating ensembles of alternative network configurations.

Quantum yield of excitation migration is not the best measure of robustness and optimality for a light harvesting system, merely the simplest one. Ideally, the aspects of regulation, synthesis, assembly, and repair of the light harvesting apparatus, as well as the processes of charge transfer and photoprotection need to be taken into account before judging the adaptability of a light harvesting system. In fact, since the dissipation rates are much lower than excitation transfer rates, excitation migration is typically not a rate limiting step in the context of the overall photosynthetic function. The quantum yields for typical chlorophyll networks as investigated above are very high and disturbances on the network usually cause only small changes on the quantum yield. Nevertheless, even with these shortcomings in mind, an investigation of the excitation migration process under the influence of external perturbations provides insights into the design principles of a light harvesting complex.

Below we present results regarding the robustness and optimality of the chlorophyll network of cyanobacterial PSI (Şener *et al*., 2002b; 2004). Similar results were also reported in (Yang *et al*., 2003).

Fig. 7 illustrates that the quantum yield of PSI changes very little through fluctuations of chlorophyll site energies nor even through selective loss of individual chlorophylls from the network. The former is a case of parameter insensitivity, while the latter illustrates the aspect of graceful degradation as two major manifestations of robustness. In the case of insensitivity to site energy fluctuations (cf. Fig. 7(a)), the consistently high quantum yields are a consequence of the broad lineshapes of pigments, which maintain significant overlap for resonant energy transfer even when chlorophyll site energies are displaced randomly. The tolerance against loss of individual chlorophylls (cf. Fig. 7(b)) is a consequence of the Förster radius being sufficiently large compared to the typical inter-chlorophyll distances. Even with the pruning of individual components, the network depicted in Fig. 5(a) maintains efficient excitation transfer. A similar result is seen for the case of simultaneous pruning of a large number chlorophylls (not shown); after taking into account the loss of the corresponding cross-section, the relative quantum yield of the pruned system remains high due to the slowness of dissipative processes. Expectedly, the highest

impact on the quantum yield results from the pruning of the chlorophylls closest to the reaction center.
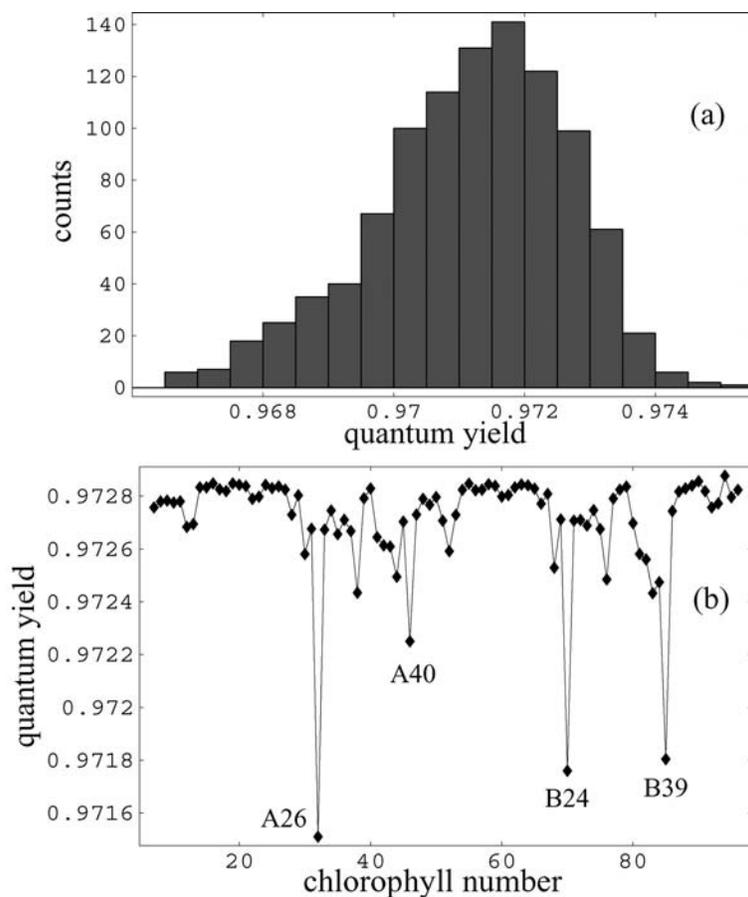
Fig 7. Robustness of the chlorophyll network in cyanobacterial PSI. (a) Robustness against fluctuations of site energies. The histogram shows the distribution of the quantum yield over an ensemble of 1000 chlorophyll configurations generated by randomly displacing the chlorophyll site energy within a width of 180 cm^{-1}. (b) Robustness against the pruning of individual chlorophylls. The average quantum yield of the remaining chlorophyll network is shown as a function of the pruned chlorophyll for all chlorophylls except for six central chlorophylls. The chlorophylls whose deletion has the highest impact on quantum yield are indicated.

Is the geometry of the chlorophyll network in PSI depicted in Fig. 5 optimized for efficient excitation transfer? Are the particular positions and orientations of individual chlorophylls critical for the light harvesting function? These questions arise naturally by contrasting the seemingly random arrangement of chlorophylls in PSI with the symmetrical arrangement of chlorophylls in LH2 illustrated in Fig. 1. The distribution of quantum yields across an ensemble of alternative network geometries generated by random reorientations of chlorophylls is given in Fig. 8. It is seen that the quantum yields vary only within a narrow interval in such an ensemble. Thus, individual chlorophyll orientations are not critical for maintaining a reasonable light harvesting efficiency. Yet within the narrow distribution of quantum yields the original configuration is seen to be nearly optimal. Constraining the random reorientations to peripheral chlorophylls (all except the six central chlorophylls that are part of the electron transfer chain) renders the optimality less prounced (Yang *et al*., 2003).

Is the apparent optimality depicted in Fig. 8 a genuine result of competitive evolution or is it only a computational artifact? It is not obvious why a difference of a percent or less in the efficiency of a process would matter for the survival of an organism. Over a sufficiently large number of generations slight reproductive advantages can be multiplied to become discriminating. Examples of competitive advantage without the display of phenotypical differences has been reported in growth competition experiments (Ouyang *et al.*, 1998). Similarly, the remarkable conservation of the geometry of the chlorophyll network in PSI in cyanobacteria and plants after 1 billion years of divergent evolution suggests that a degree of optimality was reached prior to the divergence of the two organisms.
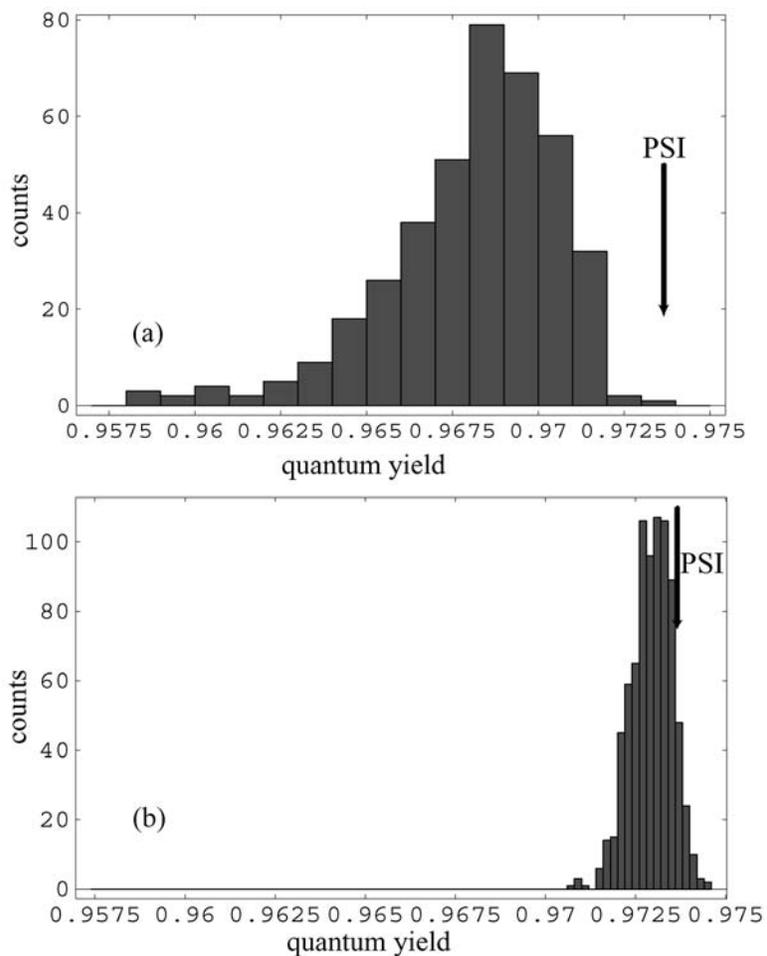
Fig 8. Optimality of the chlorophyll network of trimeric cyanobacterial PSI. Histograms show the distribution of quantum yield over an ensemble generated by randomly rotated chlorophylls. The quantum yield of the original configuration is indicated by an arrow. (a) All chlorophylls, including the reaction center chlorophylls are reoriented (400 configurations) (b) All chlorophylls other than the six central chlorophylls are reoriented (800 configurations).

7. PRINCIPLES FOR DESIGNING ARTIFICIAL LIGHT-HARVESTING SYSTEMS

The results presented above suggest certain design principles which are relevant for the design of artificial light harvesting systems. An ideal pigment network would have to be efficient at all steps of photon absorption, excitation migration, and charge transfer. Some of the design principles of an efficient light harvesting system are:

Broad absorption profile. Natural light harvesting systems contain a variety of pigments with different absorption spectra. Efficient coupling between pigments of different energies results from thermally broadened lineshapes giving rise to resonant transfer. Pigments with higher energies tend to be located further away from the reaction centers in a funnel-like arrangement (the purple bacterial photosynthetic unit is a typical example of this (Hu *et al.*, 2002)).

Efficient excitation transfer. Most of the absorbed photons result in a charge separation event in a natural light harvesting system. This high quantum yield is a consequence of the excitation transfer rates being much larger than dissipation rates. In other words, for excitation migration processes to be efficient, the Förster radius needs to be much larger than the typical inter-pigment separation.

Efficient electron transfer. Antenna Pigments are generally located far enough from the electron transfer chain to avoid a direct overlap of electronic wavefunctions. This way the loss of the transported electron is avoided.

Number of pigments per reaction center. The most efficient excitation transfer mechanism will still be wasteful if it is idle most of the time. Therefore, the number of pigments surrounding a reaction center must be chosen such that the electron transfer chain is constantly active. For example, for a charge separation time scale of 1 ms and a high light intensity of 10 photons/chlorophyll/s, on the order of 100 chlorophylls are needed to keep the reaction center supplied with electronic excitation. Monomeric cyanobacterial PSI contains 96 chlorophylls.

Robustness: Parameter insensitivity. External perturbations, such as the effects of thermal disorder, or modifications to network geometry has little effect on the overall efficiency of the light harvesting process.

Robustness: Graceful degradation. Natural light harvesting systems are tolerant to the loss of individual components. Loss of one pigment generally does not prove detrimental beyond the loss of the corresponding cross-section.

Optimality of excitation transfer network. Even though natural light harvesting systems appear to be optimized in terms of the details of their network geometry, this is probably not a high priority constraint for artificial light harvesting systems.

Protection from photodamage and repair. Natural light harvesting systems have developed mechanisms to handle excess light energy or harmful by-products of light harvesting. For example, photosystem II is known to feature a remarkable damage-repair cycle (Blankenship, 2002).

It must be noted that these principles are derived mainly from chlorophyll-based photosynthetic species and are not necessarily relevant for rhodopsin-based photosynthesis that directly couples a *cis-trans* isomerization to ion transport across the membrane.

With the availability of an increasing number of atomic resolution structures and ultrafast spectroscopy data for different photosynthetic systems, it is becoming possible to compare the details of various light harvesting mechanisms. Further modeling challenges are provided by multi-subunit light harvesting systems, where multiple protein-pigment complexes interact with one another. It is a fascinating challenge to piece together the evolutionary history of photosynthesis from comparative studies of different light harvesting systems.

ACKNOWLEDGMENTS

References

1. van Amerongen H, Valkunas L, and van Grondelle R. *Photosyntetic Excitons*. World Scientific, Singapore, 2000.
2. Ben-Shem A, Frolow F, and Nelson N. Crystal structure of plant photosystem I. *Nature* 2003; **426**:630-635.
3. Bibby TS, Nield J, and Barber J. Three-dimensional model and characterization of the iron stress-induced CP43'-photosystem I supercomplex isolated from the cyanobacterium *Synechocystis* PCC 6803. *J. Biol. Chem.* 2001; **276**:43246-43252.
4. Blankenship, R. Molecular evidence for the evolution of photosynthesis. *Trends Plant Sci.* 2001; **6**:4-6.
5. Blankenship R. *Molecular Mechanisms of Photosynthesis*. Blackwell Science, Malden, MA, 2002.
6. Damjanović A, Ritz T, and Schulten K. Energy transfer between carotenoids and bacteriochlorophylls in a light harvesting protein. *Phys. Rev. E* 1999; **59**:3293-3311.
7. Damjanović A, Kosztin I, and Schulten K. Excitons in a photosynthetic light-harvesting system: a combined molecular dynamics, quantum chemistry and polaron model study. *Phys. Rev. E* 2002; **65**:031919 - 24 pages.
8. Damjanović A, Vaswani HM, Fromme P, and Fleming GR. Chlorophyll excitations in photosystem I of *Synechococcus elongatus*. *J. Phys. Chem. B* 2002; **106**:10251-10262.
9. Dexter DL. A theory of sensitized luminescence in solids. *J. Chem. Phys.* 1953; **21**:836-850.
10. Förster T. Zwischenmolekulare Energiewanderung und Fluoreszenz. *Ann. Phys.* (Leipzig) 1948; **2**:55-75.
11. Hu X, Ritz T, Damjanovic A, Autenrieth F, and Schulten K. Photosynthetic apparatus of purple bacteria. *Quart. Rev. Biophys.* 2002; **35**:1-62.
12. Humphrey W, Dalke A, and Schulten K. VMD – Visual Molecular Dynamics. *J. Mol. Graphics* 1996; **14**:33-38.
13. Jordan P, Fromme P, Witt HT, Klukas O, Saenger W, and Krauβ N. Three-dimensional structure of cyanobacterial photosystem I at 2.5 Å resolution. *Nature* 2001; **411**:909-917.
14. Koepke J, Hu X, Muenke C, Schulten K, and Michel H. The crystal structure of the light harvesting complex II (B800-850) from *Rhodospirillum molischianum*. *Structure* 1996; **4**:581-597.

15. Ouyang Y, Andersson CR, Kondo T, Golden SS, and Johnson CH. Resonating circadian clocks enhance fitness in cyanobacteria. *Proc. Nat. Acad. Sci. USA* 1998; **95**:8660-8664.

16. Park S, Şener MK, Lu D, and Schulten K. Reaction paths based on mean first passage times. *J. Chem. Phys*. 2003; **119**:1313-1319.

17. Scheer H. (ed.) *Chlorophylls.* CRC Press, Boca Raton, Florida, 1991.

18. Şener MK, and Schulten K. A general random matrix approach to account for the effect of static disorder on the spectral properties of light harvesting systems. *Phys. Rev. E* 2002; **65**:031916 - 12 pages.

19. Şener MK, Lu D, Ritz T, Park S, Fromme P, and Schulten K. Robustness and optimality of light harvesting in cyanobacterial photosystem I. *J. Phys. Chem. B* 2002; **106**: 7948-7960.

20. Şener MK, Park S, Lu D, Damjanovic A, Ritz T, Fromme P, and Schulten K. Excitation migration in trimeric cyanobacterial photosystem I. *J. Chem. Phys.* 2004; In Press.

21. Yang M, Damjanović A,, Vaswani HM, Fleming GR. Energy transfer in photosystem I of cyanobacteria *Synechococcus elongatus*: model study with structure-based semi-empirical Hamiltonian and experimental spectral Density. *Biophys. J.* 2003; **85**:140-158.

22. Xiong J, Fischer WM, Inoue K, Nakahara M, and Bauer CE. Molecular evidence for the early evolution of photosynthesis. *Science* 2000; **289**:1724-1730.

23. Zazubovich V, Matsuzaki S, Johnson TW, Hayes JM, Chitnis PR, and Small GJ. Red antenna states of photosystem I from cyanobacterium *Synechococcus elongatus*: a spectral hole burning study. *Chem. Phys.* 2002; **275**:47-59.